Forces in Mechanics 6 (2022) 100056

Contents lists available at ScienceDirect

Forces in Mechanics

journal homepage: www.sciencedirect.com/journal/forces-in-mechanics

Comparison of local fatigue assessment methods for high-quality butt-welded joints made of high-strength steel

Moritz Braun [a,1,*], Antti Ahola [b,2], Aleksandar-Saša Milaković [a], Sören Ehlers [a,3]

[a] Institute for Ship Structural Design and Analysis, Hamburg University of Technology, Am Schwarzenberg Campus 4(C), Hamburg 21073, Germany
[b] Laboratory of Steel Structures, Lappeenranta-Lahti University of Technology LUT, Lappeenranta, Finland

ARTICLE INFO

Keywords:
Fatigue testing
Theory of critical distances
Stress averaging approach
4R method
Peak stress method
Structural hot-spot stress approach
Effective notch stress approach

ABSTRACT

Fatigue strength of welded joints is typically independent of the parent material static strength; however, there are two exceptions from this rule—post-weld treated joints and high-quality joints. The reason for both is the absence of sharp weld transitions. Thus, fatigue life is not fully governed by fatigue crack propagation but also by fatigue crack initiation. This is intensified by the fact that crack initiation behaviour is proportional to static strength properties. Commonly, this effect is not accounted for by design guidelines and typical fatigue assessment methods for welded joints. This study hence investigates the applicability and accuracy of different local fatigue assessment methods for high-quality welded joints made of high-strength steel. For this purpose, fatigue test results of S500 structural steel joints with weld toe and weld root failure are assessed using a variety of local approaches and then compared to the nominal stress approach. Finally, the transferability of results to large-scale structures are discussed and recommendations are given for practical applications.

1. Introduction

High-strength steel (HSS), or high tensile and low-carbon content steel, shows a better resistance to an applied load, i.e., in a quasistatic tensile test, per unit of weight than mild strength steel. This allows for the utilisation of less material, while reaching equal capacity. Further, high-strength steel can be used, when milder steel grade would result in unfavourable plate thicknesses and laborious welding to join thick components with multiple passes; however, the weldability of HSS may be a challenge. For cyclically loaded structures the fatigue strength becomes a design relevant issue, which must be addressed. Due to often mild steel-like fatigue behaviour of notched HSS components under cyclic loading, some kind of post-weld treatment becomes necessary in highly stressed welds to enable the full use of the higher strength. As a result, lightweight structures with a high stiffness can be design and manufactured. Another advantage of high strength steel is the possible increase in absorbed energy in a collision or crash scenario, see Ehlers [1]. Comprehensive reviews of the potentials of high-strength fine-grained steel for structural design were presented by Miki et al. [2] or van Es et al. [3].

In recent years, a number or studies assessed the applicability of HSS for engineering structures [4,5]; yet, in order to exploit the benefit of HSS excellent fabrication quality was determined to be the key element [4,6]. This might be difficult for fatigue critical welds, since the fatigue strength of welded HSS is often equal to the fatigue strength of mild steel [7], which is related to the notch-sensitivity of HSS [8]. The fatigue strength of sharply notched, e.g., welded structures is governed by earlier crack initiation relative to the number of cycles to failure. This is intensified by the fact that the fatigue crack propagation phase is, as a first approximation and simplification, independent of material strength [9]. Hence, no relation between static strength properties and fatigue strength is observed in welded specimens with sharp notches, see Maddox [7]; however, for mild notches fatigue strength increases with material strength, since crack initiation is a process governed by cyclic plasticity [10]. High yield strength consequently leads to a decreased cyclic plasticity and thereby to an extended fatigue crack initiation period, which in turn prolongs fatigue life.

The possible increase of fatigue strength for mild notches was presented in a comparison of as-welded, post-weld treated and notched base material in Braun et al. [11]. They showed, that it is possible to achieve

* Corresponding author.
E-mail address: moritz.br@tuhh.de (M. Braun).
[1] orcid.org/0000-0001-9266-1698.
[2] orcid.org/0000-0001-8706-5680.
[3] orcid.org/0000-0001-5698-9354.

https://doi.org/10.1016/j.finmec.2021.100056
Received 18 October 2021; Received in revised form 16 November 2021; Accepted 16 November 2021
Available online 26 November 2021

fatigue strength after post-weld grinding which is close to the base material fatigue strength for comparable notch severity; yet, due to the limitation to account for this positive effect of post-weld treatment in fatigue design standards, the usage of such methods is currently limited. Similarly, fatigue strength increase can not only be achieved by post-weld treatment, but also in as-welded steel joints, if high-quality welds can be fabricated. High-quality in terms of fatigue strength is generally related to low notch acuity. For notches in general, the governing parameter of notch acuity are notch radius, notch opening angle, and notch depth.

An interesting comparison between good manual arc welds and submerged arc (SAW) welded joints can be found in Maddox [7] or da Silva et al. [12] indicating that the welding process and thereby the weld quality has a significant influence on the fatigue strength and on the slope of the S-N curve. The presented difference in fatigue strength of high-quality manual arc welded joints is almost two times compared to SAW welded joints. This was simply achieved by choosing a welding process that creates weld transition with large notch radii. Such increases are, however, often limited to butt joints with mild notches (cf. [13–21]), and only if production-related defects are omitted (see [22,23]). This fact consequently hinders the beneficial usage of HSS in large-scale engineering structures, due to the large number of fillet-welded joints with high stress concentrations. Currently, a number of questions remain regarding the transferability of results obtained from high-quality small-scale test specimens to large-scale structures, see [24]. As many studies typically present results for one or two different cases (e.g. different welded joints, failure locations), questions regarding mean stress effects [25] and comparability inevitably arise [26,27].

A wide range of publications present the possible increase in fatigue strength for HSS joints [13,15,28–31] in butt-welded joints. Some design standards (e.g., DNVGL-RP-C203 [32]) permit the use of own fatigue design curves higher than those typically recommended if this effect is proven by fatigue testing; nevertheless, this effect also has to be accounted for in numerical fatigue assessment methods. Conventional stress-based fatigue assessment methods, namely the *nominal* or *structural hot-spot stress* methods are, however, not capable to do so [16,33]. On the other hand, the *effective notch stress* method seems to overestimate the fatigue strength of butt welded HSS in some cases [30].

In order to further exploit the full potential of high-quality welded joints, this study investigates the fatigue strength of high-quality welded joints by testing joints with different failure locations under the influence of different mean stresses. For this purpose, fatigue tests are performed for S500 butt-welded joints produced by flux-cored arc welding (FCAW). These results are then assessed by different fatigue assessment methods to compare their prediction accuracy for high-quality HSS butt-welded joints.

First, the test specimens are introduced and characterized in Section 2 before the results of the fatigue tests are presented and discussed in Section 3. Next, an introduction to the applied fatigue assessment methods is given in Section 4, then applied in Section 5 to assess the fatigue test results. The main focus of this section is a comparison of prediction accuracy. Finally, the results of this study are discussed with respect to transferability of large-scale structures and then recommendations are given for practical fatigue assessment of high-quality welded joints in Section 5.

2. Test specimens and setup

2.1. Mechanical properties of the S500 base material and its welded joints

The S500G1+M steel is a fine-grained thermo-mechanically rolled structural steel. The measured mechanical properties of the steel is listed in Table 1 and the chemical composition can be found in Braun et al. [34]. All specimens were saw-cut from 1 m x 0.5 m plates; welded by the FCAW process using temporary root backing [35]. Tack welds were used during welding to limit angular distortion and later removed. The plates were joined using four weld layers of Stein Megafil 821R 1.2 mm wire. The welding direction is normal to the rolling direction of the base material.

Table 1
Mechanical properties of the S500 steels [34].

	Yield strength σ_{YS} [MPa]	Ultimate tensile strength σ_{UTS} [MPa]	Elongation at fracture e_f [%]
S500G1+M	595	651	23

The S500G1+M steel has a low equivalent carbon content ($C_{eq} = 0.42$ according to EN 1011–2 [36]) and is thus not sensitive to excessive increase in the hardness at the heat-affected zone due the welding and subsequent rapid cooling; however, to confirm the requirements of DNVGL-OS-C401 [37] (hardness is limited to 420 HV for steels corresponding to DNVGL steel grades VL 460 to VL 690), hardness measurements were conducted using the HV10 technique as per EN ISO 9015–1 [38], i.e. the paths were measured in the vicinity of the top and bottom surfaces, and the intersection of weld root and weld face passes. Fig. 1 presents the results of hardness measurements. As can be seen from Fig. 1, negligibly small changes in hardness can be observed at the heat-affected zone and weld metal, compared to the base metal, confirming a good weldability of the investigated steel grade with the applied welding process.

2.2. Weld geometry properties

One half of the test specimens failed from weld toes at the top side and the other half failed from the weld root (WR) on the side of the temporary root backing. To understand the reason for this behaviour better, first the test specimen geometry and data will be presented before the actual test results in terms of stress-life (S-N) curves.

In total 83 specimens were fatigue tested. Before the fatigue tests the geometry of all specimens were measured including angular and axial misalignment as well as the local weld geometry. For the local weld geometry measurements, laser triangulation was used and the point data was analysed using the curvature method, see Schubnell et al. [39] and Renken et al. [40]. The test specimen geometry and the local weld geometry parameters are schematically presented in Fig. 2.

For a statistical presentation of the geometrical data, each specimen surface is cut into 200 slices, for which the local weld geometry is

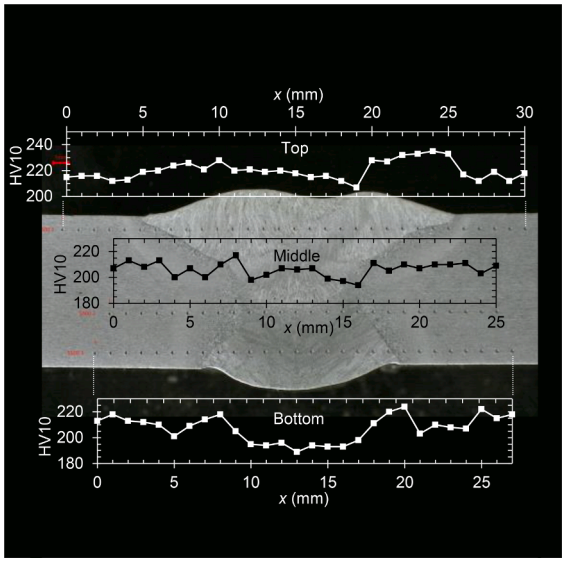

Fig. 1. Results of hardness measurements of S500G1+M 10 mm thick butt-weld joints.

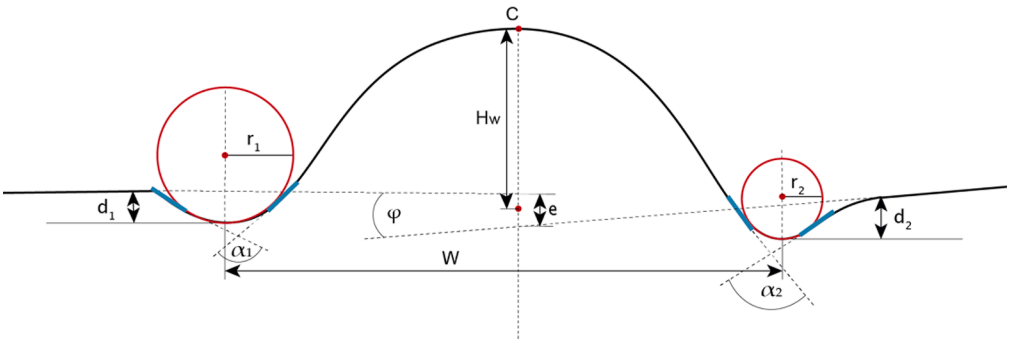

Fig. 2. Definition of test specimen geometry parameters [41].

measured. The distributions of geometrical parameters are given in Fig. 3 separately for the two failure initiation sites to allow for an assessment of results based on geometrical variations. The weld toe radii were in almost all cases larger than 1 mm and sometimes as large as 4 mm. On the other hand, weld root radii were smaller on average.

The top side notch opening angles varied between 140° and 170° for the joints failing from the WT, while the median opening angle on the WR side, was around 165° for the specimens failing the from WR. The large top side weld flank angle of the joints that failed at weld roots seems to be related to the lower weld height. In contrast, top side weld width and undercut depth are similar for both datasets. Similarly, the measurement results for all five weld geometrical features are similar on the bottom side. This is likely related to the usage of the temporary root backing.

In addition to the geometrical parameters, axial and angular misalignment of all joints was measured prior to testing. The ratio of axial misalignment to plate thickness e/t smaller than 10% for all joints. Whereas, higher variations were obtained for angular misalignment.

In summary, the S500 specimens of both series comply with class C according to ISO5817 [42]. With respect to whether failure initiated at weld toes or roots (WT or WR) on top or bottom side, the decisive factor seems to be angular misalignment. This was shown by assessing the results of a large number of fatigue tests of butt-welded joints by means of explainable machine learning, see Braun et al. [41].

2.3. Residual stress measurements

Transverse residual stresses at the plate surface, parallel to the loading direction, were measured in the selected specimen before fatigue testing using X-ray diffractometer (Stresstech G3×3000 device) with the collimator diameter of 1 mm. In the selected specimen, residual stress distributions were obtained at the weld toes and weld roots, and the results are presented in Fig. 4. The measured residual stresses were negligibly small (close to zero) but, however, it is worth mentioning that the residual stress measurements were conducted for the small-scale specimens cut from the larger welded sheet and, consequently, the potential global high tensile residual stresses have been relaxed during the specimen fabrication, and the residual stresses expectedly only includes the self-equilibrating (over the plate thickness) stress component. On the other hand, negligibly small residual stresses implies that the applied stress ratio might have a definite influence on the fatigue capacity in the joints in the as-welded condition. The reason for the compressive residual stresses on all four sides is thought to be related to the clean blasting of the plates before welding.

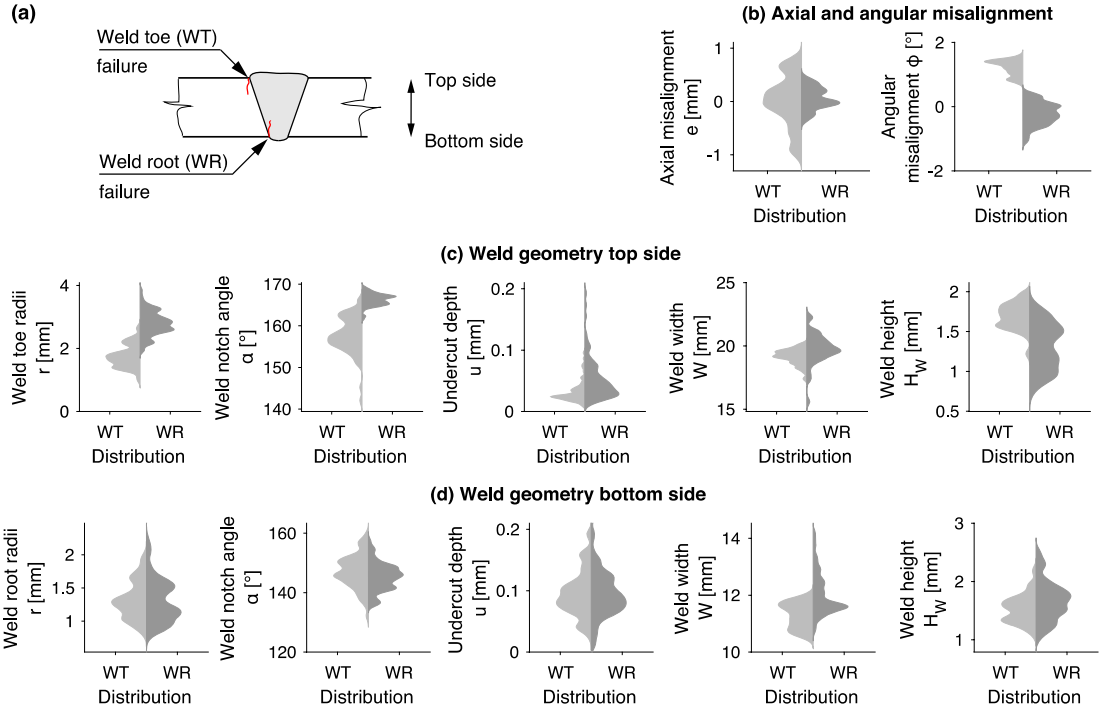

Fig. 3. Definition of weld toes and roots of one-sided but-welded joints (a), distribution of misalignment of joints (b), and of geometrical measurements results separated for the joints failing at weld toe and root, and for (c) top side and (d) bottom side.

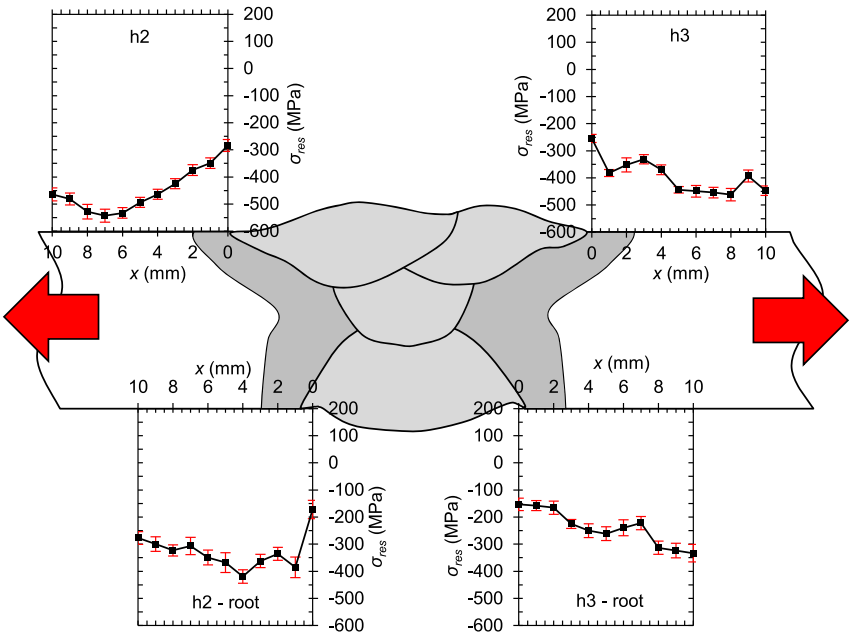

Fig. 4. Residual stress distributions at the weld toe and weld root with loading direction indicated by arrows.

3. Fatigue test results and evaluation

For this study, fatigue tests performed from previous studies [43,44] were extended and accompanied with additional investigations. For this purpose, fatigue tests were carried out under axial loading on a horizontal resonance testing machine at a frequency around 33 Hz and for two stress ratios ($R = 0$ and $R = 0.5$). Failure is defined as full fracture of a specimen. One-sided V-type butt welds may fail from two sides of the joint. The first being the WT between the heat-affected zone and the weld metal of the top weld layers and the other being the WR adjacent to the root weld layer. According to the recommendations of the International Institute of Welding (IIW) [45] weld toe failure in butt joints welded in flat shop position with a weld height below $0.1t$ is associated with a fatigue design class (FAT) FAT90, while fatigue strength of weld root failure in joints welded on temporary root backing is evaluated using FAT80 class. Herein, the number behind the abbreviation refers to the reference fatigue strength at 2 million cycles for a probability of survival of 97.5%. The nominal stress results are presented in Fig. 5.

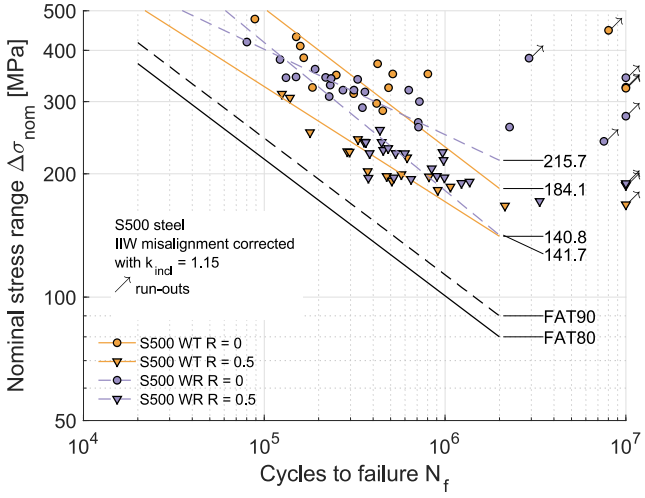

Fig. 5. S-N diagram of S500G1+M butt-weld specimens with corresponding FAT90 and FAT80 weld detail classes for weld toe and weld root failure with tabulated results and mean fatigue strength curves. Data partially taken from [43,44].

As can be seen from Fig. 5, the fatigue strength of the S500 butt-welded joints that failed from weld toes is generally higher than those that failed at weld roots. This is not surprising, as the joints that failed at WRs have a higher notch acuity (smaller notch radii and opening angles). Furthermore, all test series significantly exceed the FAT classes according to the IIW recommendations [45]. This is thought to be related to the generally large weld toe radii produced by the FCAW process.

All run-outs of S500 specimens are associated with WT or WR failures based on the angular misalignment direction and thereby the expected failure location. In general, only three specimens failed beyond 2 million load cycles and in both cases the test frequency of the resonance machine indicated a crack initiation by a reduction of test frequency in the range of 0.05 Hz. Some tests are terminated if no change of test frequency was detected at 2 million cycles or correspondingly at higher numbers of load cycles. The tests that failed after 2 million load cycles were removed from the S-N curve calculation due to the fact that they lie beyond the knee-point usually associated with S-N curves of welded joints and that one point per test series is thought to be not enough data for a test evaluation based on a maximum-likelihood algorithm. Moreover, it increases the conservatism close to the knee-point, since the slope would be shallower if they are included. In addition, base materials and specimens with low stress concentrations are usually associated with a knee point at 1 million cycles already, see Dowling [9]. The test specimens in this case are welded; however, they clearly exceed the fatigue strength usually expected for welded joints, leading to the conclusion, that the knee point might be below 2 million cycles. Defining a knee point for these specimens according to common practice for welded joints, seems uncertain based on the available data.

In Fig. 6, fracture surfaces are presented for one specimen with WT and one with WR failure. From the fracture surface, it can be seen that several fatigue cracks initiated at both failure initiation sites, which then quickly coalesced to long cracks.

Due to the high-quality of the S500 HSS joints, the reference fatigue strength $\Delta\sigma_{R,97.7\%}$ of all test series lies well above the corresponding fatigue design class. This is also related to shallower S-N curve slopes, which is an indication of a significant fatigue crack initiation phase and typical for specimens with low stress concentrations. It is typically assumed that the slope of S-N curves of welded joints is equal to the

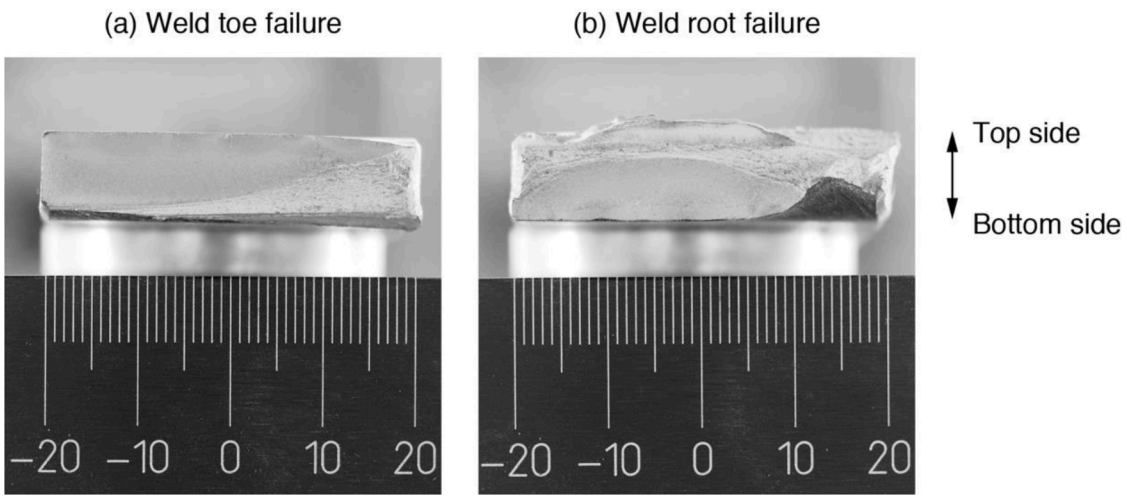

Fig. 6. Fracture surface of S500G1+M butt-weld specimens with (a) weld toe and (b) weld root failure, and scale in millimetres.

slope of fatigue crack growth curves of approximately $k = 3$ [7]. There are two test series (WT failure and $R = 0$, and WR failure and $R = 0.5$) with slopes close to this typically assumed value; however, the high standard deviation of the slope exponent SD(k) for these two test series and the large deviation between the mean strength $\Delta\sigma_{R,50\%}$ and the run-outs indicates that the actual slope is more shallow. In average, a slope exponent of $k = 4$ seems to be more suitable for the analysed welded joints. This also agrees with findings from other studies, cf. [6,12,18,20,29,30,46]. For comparison, results obtained for free and fixed slope exponents are summarized in Table 2.

Based on the difference between the test results for stress ratios $R = 0$ and $R = 0.5$, and the residual stress measurements, which showed low negligible residual stresses, the recommended reduction factor $f(R) = 1.2$ to transfer results from $R = 0$ to $R = 0.5$ [45], seems reasonable.

4. Fatigue assessment methods considered to determine fatigue strength of high-quality HSS joints

Eight different stress-based fatigue assessment methods are applied to assess the fatigue strength of the high-quality HSS joints in this study. The aim of this study is to determine, which methods are suitable to accurately predict fatigue strength of high-quality joints in the high-cycle fatigue regime without major defects. For such joints, applicable methods are limited to stress- and strain-based methods. Fracture mechanics methods typical assume initial defects. This approach is inaccurate for defect-free high-quality joints.

To reach the aforementioned goal, first a short explanation is given on how misalignment effects were considered in the assessment, before the different methods are briefly summarized and applied to assess the test data in Section 5.

4.1. Consideration of misalignment effects during fatigue assessment

Relevant for welded joints are two different types of misalignment, i. e., axial and angular. Both types cause secondary bending stresses, which affect local stress states at welds. The stress concentration factor $k_{m,e}$ based on the ratio of axial misalignment e to plate thickness t can easily be calculated according to Niemi et al. [47] with Eq. (1).

$$k_{m,e} = 1 + 3\frac{e}{t} \tag{1}$$

Contrary to the secondary bending effect due to axial misalignment, the effect due to angular misalignment is dependent on the applied external loading, see Eqs. (2) and (3). Under tensile loading the specimen is straightened, which is included in the misalignment calculation of different standards by a $\tanh(\beta)/\beta$ term, with the dimensionless variable β being a function of the specimen slenderness ratio (length l over thickness t), the applied nominal stress σ_{nom} and the Young's modulus E. This effect is particularly pronounced for thin ($t \leq 10$ mm) butt-welded joints [48,49].

$$k_{m,a} = 1 + \frac{3\varphi}{2}\frac{l}{t}\frac{\tanh(\beta/2)}{\beta/2} \tag{2}$$

$$\beta = \frac{l}{t}\sqrt{\frac{3\sigma_{nom}}{E}} \tag{3}$$

Misalignment effects are known to affect fatigue life assessment and are thus considered in this study. To this end, secondary bending stresses caused due to axial and angular misalignment are superimposed on the applied membrane loading during finite element (FE)-based fatigue assessment. This will subsequently be presented for the structural hot-spot stress extrapolation method.

4.2. Structural hot-spot stress extrapolation method

The calculation of different stress components allows a superposition of the different stress components in a half model of the butt welded joints (see Fig. 7), which significantly reduces the computational effort [50]. Here the components are applied 3t away from the weld toe. In

Table 2
Fatigue stress results for a stress ratio $R = 0$ with calculated fatigue strength $\Delta\sigma_{S_R}$ at $N = 2{\cdot}10^6$ for 50% and 97.7% survival probability, evaluated using a free and a fixed slope exponent $k = 4$.

Failure location	Stress ratio	Free slope k					Fixed slope k			
		k	SD(k)	$1 : T_s$	$\Delta\sigma_{R,50\%}$	$\Delta\sigma_{R,97.7\%}$	k	$1 : T_s$	$\Delta\sigma_{R,50\%}$	$\Delta\sigma_{R,97.7\%}$
WT	0	3.0	0.92	1.51	184.1	133.4	4	1.38	218.3	169.7
	0.5	3.6	0.43	1.21	140.8	121.0	4	1.20	148.0	128.7
WR	0	4.8	0.70	1.19	215.7	188.0	4	1.25	198.5	167.2
	0.5	2.8	0.94	1.39	141.7	109.4	4	1.27	160.9	133.3

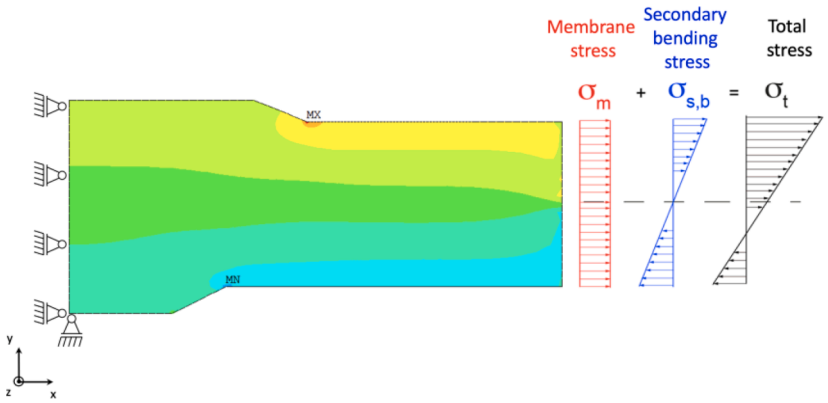

Fig. 7. Structural hot-spot stress model presenting the bending stress distribution in lateral direction x (here $\sigma_m = 0$ for visualisation purposes of the bending stress distribution) on the left and stress component superposition on the right.

order to create the presented though-thickness bending stress profile, two contrary forces are applied at the upper and lower half of the free edge to the right. Those forces are calculated from beam theory and cause only a localised stress concentration at the free edge, see Fig. 7.

The effect of the applied forces decays around 0.5t from the free end of the model. Moreover, by applying only a bending stress it is confirmed that the bending stress is almost constant between 0.4t and 1t on upper side with a deviation less than 0.5%. The deviation on the lower side is slightly larger, but this is related to the change in cross-sectional area close to the weld root.

In order to simulate the large amount of test specimens, an automated analysis procedure was created by coupling Matlab and ANSYS. Here, the specimens of one test series are modelled with the median geometrical dimensions and plane strain quadratic elements. A similar approach was chosen by Gaspar et al. [51], who analysed the effect of weld imperfections on structural hot-spot stress assessment by assuming a normal distribution of geometry parameters, or by Lillemäe et al. [33], who investigated the effect of weld quality on fatigue strength of butt-welded joints. The here presented approach to consider misalignment effects was then adopted for the other fatigue assessment methods in the current study.

For weld toe failure assessment of butt-welded joints, FAT100 class is recommended. According to the IIW recommendations [45], the term weld root is used for weld transitions at single-sided butt-welded joints on root backing. Typically, fatigue assessment theories use this term only for notches created at non-fused parts of welded joints, e.g., roots of non-penetrating cruciform or butt-welded joints with opening angles $\alpha \rightarrow 0°$. In this study, weld root is used to distinguish the top and bottom side of the single-sided butt joints.

4.3. Xiao and Yamada's 1 mm stress approach

Another structural stress approach is Xiao and Yamada's *1 mm stress* approach [52]. The underlying idea is that the non-linear stress increase decays 1 mm from a local stress raiser, i.e., weld toe or weld root. For weld toe failure, it is recommended to use the stress component parallel to the direction of applied loading and elements with quadratic shape function as large as 0.5 mm [53].

The 1 mm stress approach was found to be non-conservative for thin welded joints due to the steep gradient in through thickness direction [27]; however, it is well suited for moderate to thick plates ($t \geq 8$ mm) [54]. For weld toe failure assessment of such joints, the FAT100 class is recommended.

4.4. Effective notch stress method and theory of critical distances

The structural stress concepts often prove to be conservative for butt joints of higher-strength materials, since this concept, like the nominal stress concept, has been calibrated for the most part on the basis of test specimens which have a predominant crack growth phase. As can be seen from strain gauge measurements, significant crack initiation phases can occur in high-strength notched specimens or mildly notched welded joints with large weld transition radii [55,56], which is why both the nominal and the structural stress concepts underestimate their fatigue strength. Another concept included in fatigue design rules is the effective notch stress approach.

In general, notch stress concepts are potentially better suited to assess local notch effect, because the local weld geometry is taken into account and the failure relevant stress is evaluated directly at the highest loaded point. In welded structures, sharp notch radii often occur at weld toes or roots. Thus, the effective notch stress (ENS) concept according to Radaj et al. [10] is based on the assumption of negligible notch radii $r_{real} \rightarrow 0$ mm, see Eq. (4). Thereby a fictitious enlargement of the notch radius to $r_{ref} = 1$ mm was proposed for a micro-structural support length of $\rho^* = 0.4$ mm (assuming a cast iron-like structure in the heat affected zone) and a factor $s = 2.5$ for the multiaxial stress state at the notch.

$$r_{ref} = r_{real} + s\rho^* \tag{4}$$

The replacement of the weld radii with a fictitious reference radii $r_{ref} = 1$ mm is usually not recommended for weld details having small stress concentration ($K_t < 1.6$), see Fricke [57]; nevertheless, Pedersen et al. [58], and Rother and Fricke [59] showed that the effective notch stress approach can be applied to welds having low stress concentrations. For such welds, an additional check of the fatigue strength of the base material is required. For example, the results of Collmann and Schaumann [60] for 30 mm SAW butt welded joints are clearly above the corresponding nominal stress FAT curve, but fall below the FAT225 curve of the effective notch stress approach due to the low stress concentration of the test specimens.

For mild notches with real radii $r_{real} > 1$ mm, the application is difficult or may even lead to non-conservative results. An application of actual radii would be conceivable for this application, but seems impracticable due to the large range of possible notch radii. It will thus be tested if the application of $r_{ref} = 1$ mm is suitable for HSS butt joints with low stress concentrations.

Alternatively, effective notch stress concepts can be applied as these are able to directly account for support effects at notches. Examples of such methods include Neuber's *stress averaging* approach [61], Peterson's *critical distance* approach [62], or Taylor's *Theory of Critical Distances* (TCD) [63], who harmonized different effective stress methods such as the two aforementioned. The basis of such methods is the determination of an effective stress, which takes into account the notch geometry, as well as the micro-structural support effect of the surrounding material. This is achieved by averaging the stress gradients along the anticipated crack path (or notch bisector) or at a certain depth

(critical distance). For simplicity, the stress gradient is often evaluated perpendicular to the surface from the point of the maximum principal stress, as can be seen from Fig. 8.

The averaged stress is then obtained by averaging over the length of ρ^*, see Eq. (5). Alternatively, the effective stress is determined as the stress in a distance a from the notch tip. It is often assumed that both yield similar results for $\rho^* = 4a$ [64,65]. As mentioned earlier, $\rho^* = 0.4$ mm for welds is based on the assumption that the microstructure of welds resembles cast iron. Recent studies, however, show that the micro-structural support length ρ^* depends not only on the static strength of the material, but also on the notch acuity [66–68], because in the case of welds with sharp notches the value of 0.4 mm has been confirmed for a large number of materials, while Baumgartner et al. [69] and Braun et al. [70] showed a clear material strength dependence for post-weld treated joints with smooth weld transitions.

$$\sigma_{eff} = \frac{1}{\rho^*} \int_0^{\rho^*} \sigma(x) \mathrm{d}x \tag{5}$$

By considering the weld geometry in the microscale Liinalampi et al. [71] found a very small micro-structural support length $\rho^* = 0.05$ mm for laser-hybrid welds made from thin plates. The consideration the geometrical variation in the micro-scale allows high accuracy modelling of the measured weld toe radii; however, the definition of radii and weld flank angle for fatigue assessment is an on-going debate and currently the topic of on-going research, see Schubnell et al. [39]. For this study it is therefore decided to use a constant fictious reference radius of $r = 0.05$ mm, as well as $\rho^* = 0.4$ mm and $a = 0.1$ mm, which also allows use of recommended FAT160 design curve, see Baumgartner [72].

The weld toe and root radii have been modelled with a constant number of 5 elements along the radius, which was found to yield an effective stress for an averaging length $\rho^* = 0.4$ mm which is only 1% smaller than the converged effective stress [67].

4.5. Peak stress method

Neuber's idea of a micro-structural support effect at notches led to the development of various fatigue assessment methods. One of those is the *peak stress* method. The peak stress method is further based on the *notch stress intensity factor* (NSIF) concept and the *averaged strain energy density* (ASED) method.

Again, assuming a vanishing weld toe radius it can be shown that the asymptotic stress field can be described based on Williams' stress field solution [73]. In order to quantify the size of this zone for fatigue assessment, the NSIF concept was introduced [74]; however, the NSIF is computationally cumbersome and not applicable for 3D structures. Thus, the ASED method was introduced to simplify fatigue assessment [75]. Similar to the stress averaging approach, a fatigue-effective quantity is derived by averaging the strain energy density in an area around weld toes or roots; nevertheless, a particular mesh refinement and the definition of a control area is required. Hence, Meneghetti and Lazzarin [76] proposed a coarse mesh refinement with 1 mm elements in order to obtain peak stresses at fatigue relevant locations. Using the relation between the peak stress at sharp V-type notches and the mode I NSIF, they provided a fast and easy to apply method to determine the averaged strain energy density for a given control radius and notch opening angle. Alternatively, the obtained peak stress range can directly be applied for fatigue assessment. For this purpose, a design curve FAT156 was proposed for fatigue failure of welded structural steel joints in recent years [77,78]. Clearly, there are certain limitations with respect to the definition of sharp V-type notches at weld transitions. According to Meneghetti et al. [77], weld transition radii should be smaller than 2 mm. As the median radii of the joints of this study are smaller than 2 mm (the critical radii are even smaller) at the failure initiation locations (WT or WR), this condition is fulfilled and the method should be applicable.

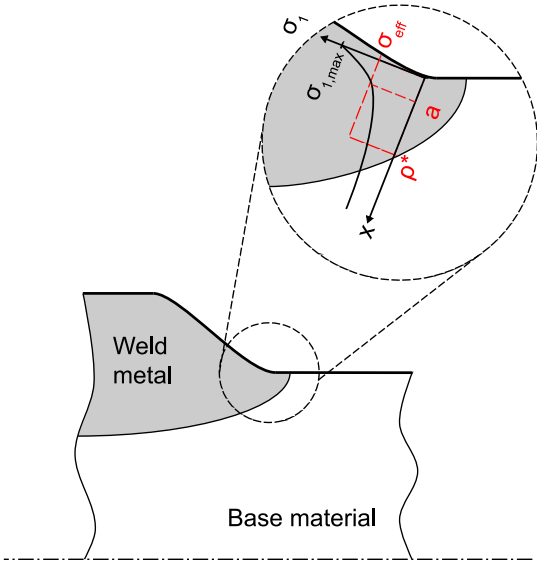

Fig. 8. Schematic illustration of the application of the stress averaging and critical distance approach at weld toes of butt joints.

4.6. 4R method

In the above-described local approaches, the main concern is to consider mean stress corrections in the fatigue assessments in the joints with the low or compressive residual stresses, for instance due to the post-weld treatments, and different applied stress ratios of external loading. To address this aspect, Nykänen and Björk [46] developed an approach in which the ENS concept is associated with the Smith-Watson-Topper mean stress-correction, employing butt weld fatigue test data. At that time, the approach was called the *3R* method as per the three parameters—the residual stress (σ_{res}), applied stress ratio (R) and material ultimate tensile strength (R_m), included in the analysis. Further research extended its use for the geometrically improved joints, such as TIG-dressed [79] and ground [80] joints, and consequently, actual notch radius (r_{real}) was implemented in the model, and the approach was named as the *4R* method with the additional parameter. In the 4R method, the ENS is calculated on the basis of $r_{real} + 1$ mm concept, and utilizing the computed linear-elastic ENS, the elastic-plastic stress-strain behaviour at the notch root is analytically simulated employing Neuber's concept for correcting elastic stresses for the plasticity. As a result from the stress-strain behaviour, the local maximum and minimum stresses are obtained, and the mean stress correction is conducted for the ENS using the local stress ratio, $R_{local} = \sigma_{\min}/\sigma_{\max}$ as follows:

$$\Delta\sigma_{4R} = \frac{\Delta\sigma_{ENS}}{\sqrt{1 - R_{local}}} \tag{6}$$

where $\Delta\sigma_{4R}$ is the mean stress-corrected ENS range, $\Delta\sigma_{ENS}$ is the (linear-elastic) ENS range. The concept of the 4R method is described more comprehensively in Ahola et al. [81]. In the current study, the design curve derived in Ahola et al. [80] (FAT288 with $k = 4.86$) is adopted, as it also considers actual weld transition radii.

5. Comparison of different fatigue assessment concepts

By applying a unit membrane and bending stress to the FE models, stress concentration factors are calculated for each fatigue assessment concept. The calculated stress concentration factors and corresponding fatigue design curves (given by the characteristic fatigue strength FAT) are listed in Table 3. The stress result of each specimen is thus obtained

Table 3
Summary of calculated stress concentration factors for tension and bending loading ($K_{t,t}$, $K_{t,b}$) separated by failure location (WT, WR), and corresponding fatigue design curves ($P_s \approx 97.5\%$, $N = 2{\cdot}10^6$) and slope exponent k.

Assessment method	Fatigue design curves	Slope exponent k	Weld toe		Weld root	
			$K_{t,t,WT}$	$K_{t,b,WT}$	$K_{t,t,WR}$	$K_{t,b,WR}$
Nominal	FAT90/FAT80	3	1.00	1.00	1.00	1.00
Hot-spot stress extrapolation	FAT100	3	1.00	1.22	1.21	0.80
1 mm concept	FAT100	3	0.99	0.79	1.11	0.65
Peak stress	FAT156	3	1.01	1.06	1.63	1.15
ENS	FAT225	3	1.77	1.78	2.32	1.72
4R	FAT288	4.86	1.57	1.55	2.06	1.53

by multiplying the acting stress with the corresponding stress concentration factor for each method and the ratio between membrane loading and secondary bending stress. Only for the stress averaging and critical distance approach, effective stress ranges were directly obtained from the FE models to ensure accurate determination of stress gradients under combined membrane and secondary bending loading. The obtained S-N results for all eight methods are presented in Fig. 9 together with the corresponding fatigue design curves.

Differences in prediction accuracy of the different methods are clearly visible from Fig. 9, i.e., difference between the accuracy for the two failure initiation locations (WT and WR). To further assess the accuracy of the fatigue assessment methods, the deviation between the experimental and the predicted number of cycles to failure for a probability of survival of approximately 97.5%, according to Eq. (7), are presented in Fig. 10. It is expected that some design curves were derived based on the mean S-N curves minus two standard deviations (corresponding to a survival probability of 97.7%) [26]; nevertheless, it is typically assumed that the difference between both approaches is negligible, see Hobbacher [45].

$$\mathrm{dev} = \log N_{f,exp} - \log N_{f,pred,97.5\%} \tag{7}$$

Besides the deviation between experimental and predicted number of cycles to failure for each test, Fig. 10 displays a histogram of all deviations and separate markers for the average deviation for both failure locations to highlight the difference in prediction accuracy. Interestingly, some methods lead to similar mean deviations for both failure locations (e.g., the hot-spot stress extrapolation method or Xiao and Yamada's 1 mm concept), while others lead to large differences such as the peak stress method. In order to quantify the mean deviation and the corresponding quantiles for both failure locations and a combined assessment, the results are displayed next in terms of box plots in Fig. 11. Here, the box corresponds to the first and third quantile (25% to 75% of sample data) and the whisker to the 0th and 100th percentile excluding assumed outliers. To determine possible outliers, the actual data is plotted besides the boxplots. As can be seen from Fig. 11, there are typically only one or two results considered to be outliers. This is thought to be related to the change of slope exponent around the knee-point of the S-N curves. Thus, results that fail in this region lead to large deviation between experimental and predicted number of cycles to failure, cf. Fig. 9 and Fig. 10. As these do not influence the median deviation much (they are not considered outliers in all comparisons), they were not excluded from the presentation.

In summary, the median deviation is typically higher for the joints that failed at weld roots. This is thought to be related to the change in cross-sectional area of the single-sided weld. Furthermore, the lowest median deviation is obtained for the effective notch stress method for both failure initiation locations and the combined assessment. Interestingly, the hot-spot stress approach leads to the highest combined deviation of all methods followed by the nominal stress approach. Difficulties in assessing mild notches by the hot-spot stress extrapolation approach are already known [69]. The other methods lead to comparable results.

In the following section, the results are first discussed with respect to transferability to large-scale structures and then recommendations are given for local fatigue assessment of high-quality welded joints.

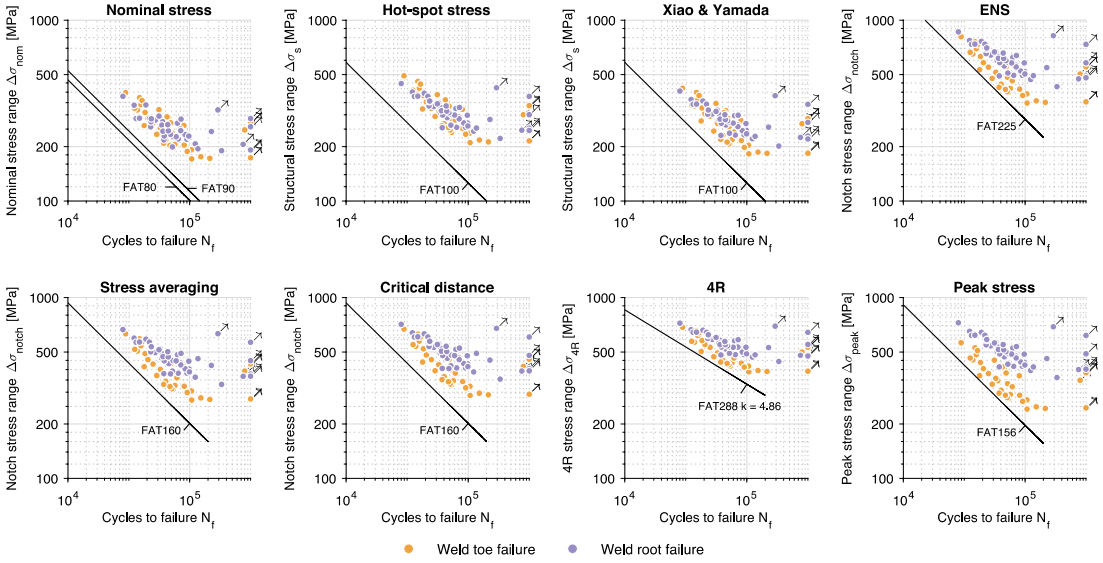

Fig. 9. Fatigue assessment results S500G1+M butt-weld specimens with corresponding design curves. All results are corrected to a stress ratio $R = 0.5$ with $f(R) = 1.2$ except those for the peak stress method (the design scatter band of this method is defined for $R = 0$).

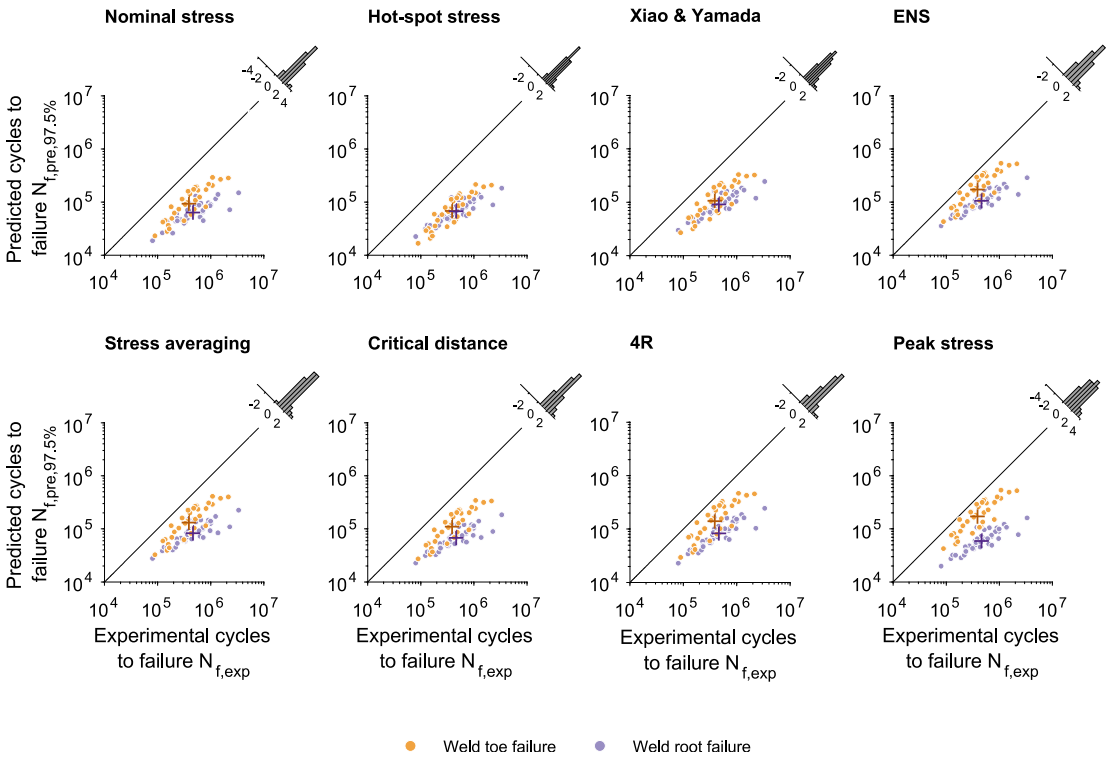

Fig. 10. Comparison of experimental and predicted number of cycles to failure based on corresponding fatigue design curves for the different fatigue assessment methods with marker for the average deviation for both failure locations and the distribution of logarithmic deviation of all test specimens. All results are corrected to a stress ratio $R = 0.5$ with $f(R) = 1.2$ except those for the 4R method (includes mean stress correction as per Eq. (6)), and for the peak stress method (the design scatter band of this method is defined for $R = 0$).

6. Discussion

6.1. Transferability of small-scale test results to large-scale structures

In recent years, several studies have been performed on fatigue strength of thin ($t \leq 10$ mm) high-strength steels joints, which often reported a shallower slope and high fatigue strength at 2 million cycles [13–17]. Herein, both quantities are often associated with high-quality welds. Remes et al. [16] for example predicted the slope of butt-welded thin steel joints for different qualities levels in terms of undercut depth and weld flank angle. Nykänen et al. [29] and Ottersböck et al. [18] tested S1100 ultra high-strength steel made by different welding techniques and related the higher fatigue strength and slope to different weld qualities and lower levels of axial misalignment, respectively; however, Nykänen et al. [29] point out, that any fatigue strength benefit compared to mild steel can only be achieved, if crack-like defects can be omitted. This leads to the conclusion, that the global and local weld geometry in terms of misalignment and notch severity is the main factor governing fatigue strength in any high-quality weld.

It is important to keep in mind that the transferability of results achieved with small scale and thin specimens to thick plates is sometimes difficult, due to scale effects that have to be considered [24]. Interestingly, Remes et al. [16] found no difference between thin small- and full-scale test specimens, leading to the conclusion, that not the width of the specimen is governing the slope, but rather the thickness of the welded steel plates. Giving explanations for the often shallower slope found in S-N tests of thin plated structures is outside the scope of this article, but shallower slopes were also for thicker SAW butt-welded joints, see Schaumann and Collmann [19] for example, finding slopes close to $k = 5$; however, in another study on 80 mm thick SAW welded HT40 butt joint specimens a slope around $k = 3$ was found [5]. Comparing the local weld geometry, it seems that the test specimens of von Selle et al. [5] had sharper notches than those of Schaumann and Collmann [19].

Another important factor which has to be taken into account for fatigue assessment of small-scale specimens is the residual stress releave due to cutting of the specimens. Since fatigue design curves are derived for thick-walled components with high tensile residual stresses. It is often assumed that, the production of small-scale specimens relieves residual stresses to some extent. Fatigue design standards therefore recommend a reduction factor $f(R) = 1.2$ to yield comparable results to the fatigue design curves based on $R = 0.5$, see Hobbacher [45]. According to Sonsino [25], this often leads to conservative results for design; nevertheless, generalisation is difficult and design standards have to ensure high reliability. Deviation from this correction factor are possible, if the presence of tensile residual stresses can be proven [45]. In the current study, negligible residual stresses were measured after specimen cutting. The IIW recommendation [45] with a reduction factor $f(R) = 1.2$ was thus adopted.

6.2. Recommendations for local fatigue assessment of high-quality welded joints in practise

In order to give recommendations for local fatigue assessment methods of high-quality welded joints in practise, the results of the comparison of the applied methods are subsequently discussed and some general remarks are given.

As expected based on previous work by Remes and co-workers [16, 33], the nominal and structural hot-spot stress extrapolation methods significantly underestimate the fatigue strength of the S500 high-quality butt joints tested for the current study. The reason for this is that these two methods are not sensitive to variations of local weld geometry. Similarly, the peak stress method only accounts for variations of opening angles at weld transitions. Due to the underlying assumption of pointed V-type notches, variations of weld toe radii cannot be accounted for by

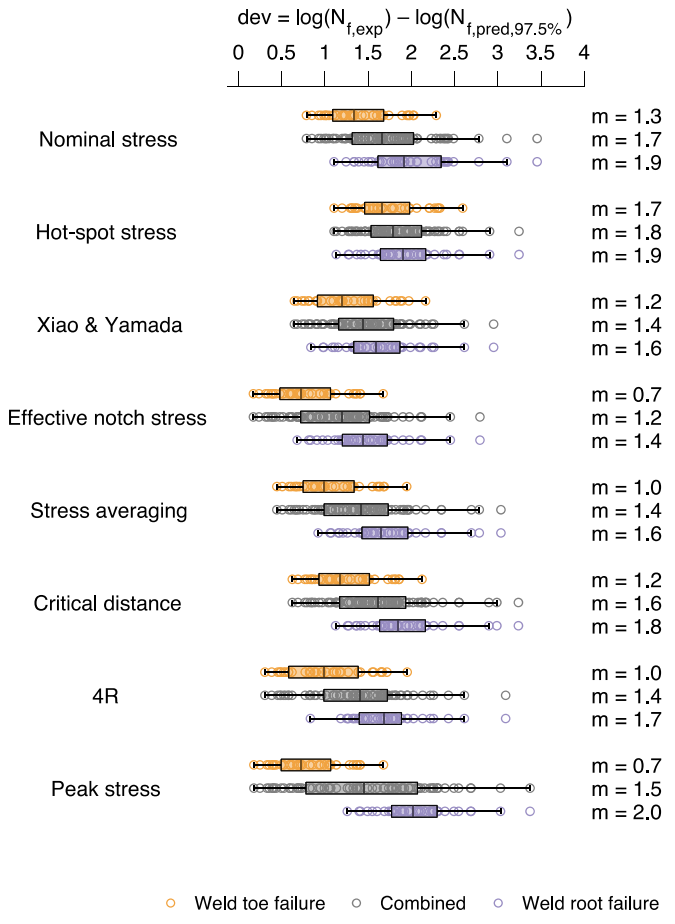

Fig. 11. Assessment of logarithmic deviation between experimental and predicted number of cycles to failure based on corresponding fatigue design curves with determined median deviation (m) for WT, WR, and combined failure. All results are corrected to a stress ratio $R = 0.5$ with $f(R) = 1.2$ except those for the 4R method, and the peak stress method (the design scatter band of this method is defined for $R = 0$).

this method. In addition, more research is required on the applicability of the peak stress method for high-quality welded joints. It is currently unclear why the method is accurate for the joints that failed at weld toes and less accurate for the joints that failed at weld roots. This could be related to the change in cross-sectional area of the single-sided weld or the aforementioned difference in weld transition radii (about 1.7 mm and 1.2 mm at WT and WR, respectively). Interestingly, the structural hot-spot stress extrapolation method seems to be less sensitive to this effect.

The majority of the other methods lead to similar prediction accuracy with the exception of the effective notch stress method, which yields the best results of all methods. Better results might be achieved for the stress averaging and critical distance approach if the actual weld geometry is considered instead of a constant fictious reference radius of $r = 0.05$ mm; yet, for this study the recommendation by Baumgartner et al. [65] was applied to be able to compare the results with their fatigue design curve FAT160. Using actual weld transition radii would require to determine a new design curve first. In addition, previous studies investigated the possibility to include material strength corrections for the stress averaging approach, see Baumgartner et al. [69] and Braun et al. [70]. This could lead to even better results for TCD methods.

In summary, the direct application of the effective notch stress method can be recommended for high-quality joints made of HSS. Typically, for such joints a check of the base material is required due to low stress concentration factors ($K_t < 1.6$), see Fricke [57], Pedersen et al. [58], and Rother and Fricke [59]. For high strength material, it can generally be assumed that the fatigue strength of base material exceeds the corresponding design curve FAT160. This, nevertheless, requires a sufficient surface quality without marks or scratches.

Some design standards (e.g., DNVGL-RP-C203 [32]) permit the use of own fatigue design curves higher than those typically recommended. This, however, requires a verification by experiments with test specimens, which are representative for the actual fabrication and construction [32]. The reason for this is that the possibility of production-related defects as well as fabrication tolerances have to be accounted for. High-strength butt-welded joints are for example prone to defects such as undercuts, see [22,23]. To be able to exploit the benefits of high-quality joints made of high-strength steel, a strict quality control is inevitable. Otherwise, there is a high risk of low fatigue life due to overestimated fatigue strength.

7. Conclusions

This study investigated the fatigue strength of high-quality welded joints made of high-strength steel. In addition, the prediction accuracy of different fatigue assessment methods for such joints was determined. For this purpose, fatigue tests on S500G1+M steel joints with weld toe and root failure at different stress ratios ($R = 0$ and $R = 0.5$) were performed. From the investigation, the following conclusions are drawn:

- Due to the high-quality of the S500 HSS joints, the fatigue strength of all test series (both failure initiation locations and stress ratios) lies well above the corresponding fatigue design classes. This is also related to shallower S-N curve slopes, which is an indication of a significant fatigue crack initiation phase and typical for specimens with low stress concentrations.
- Large differences in prediction accuracy are found for all local fatigue assessment concepts and the nominal stress approach. All concepts are leading to conservative assessment results; however, for some methods the results are overly conservative.
- In general, the higher deviation between experimental and predicted fatigue strength for weld root failure is thought to be related to the change in cross-sectional area of the single-sided weld.
- The nominal and structural hot-spot stress extrapolation methods significantly underestimate the fatigue strength of the S500 high-quality butt joints. This agrees well with previous studies by Remes and co-workers [16,33].
- In general, local fatigue assessment methods perform better than the two aforementioned methods. The highest prediction accuracy was observed for the effective notch stress method. The other local methods (Xiao and Yamada's 1 mm concept, 4R method, peak stress method, stress averaging and critical distance approaches) led to similar prediction accuracies.
- Future work could focus on the consideration of actual weld geometries and material strength in assessment procedures. For the current study, median geometry measurement results were used to build FE models; however, fatigue cracks typically initiate at the location of highest stress concentration. Further improvements could be related to the consideration of material strength correction as presented in Baumgartner et al. [69] and Braun et al. [70].

Declaration of Competing Interest

The authors declare no conflict of interest.

Acknowledgment

The authors would like to thank Shi Song and Sarah Schreiber for performing the geometry measurements of the specimens tested during this study.

References

[1] S. Ehlers, A particle swarm algorithm-based optimization for high-strength steel structures, J. Ship Prod. Des. 28 (2012) 1–9, https://doi.org/10.5957/Jspd.28.1.110029.

[2] C. Miki, K. Homma, T. Tominaga, High strength and high performance steels and their use in bridge structures, J. Constr. Steel Res. 58 (2002) 3–20, https://doi.org/10.1016/s0143-974x(01)00028-1.

[3] S. van Es, H. Slot, H. Steenbergen, J. Maljaars, R. Pijpers, Use of HSS and VHSS in steel structures in civil and offshore engineering, Steel Constr. 11 (2018) 249–256, https://doi.org/10.1002/stco.201800018.

[4] O. Doerk, S.B. Shin, G.B. An, Design impact of fracture mechanics properties of high toughness YP47 welds, in: Proceedings of the 24th International Ocean and Polar Engineering Conference, Busan, Korea, 2014.

[5] H. von Selle, O. Doerk, J.K. Kang, J.H. Kim, C. Guedes Soares, W. Fricke, Fatigue tests of butt welds and plates edges of 80mm thick plates. Advances in Marine Structures, 2011, pp. 511–519.

[6] B. Möller, J. Baumgartner, R. Wagener, H. Kaufmann, T. Melz, Low cycle fatigue life assessment of welded high-strength structural steels based on nominal and local design concepts, Int. J. Fatigue 101 (2017) 192–208, https://doi.org/10.1016/j.ijfatigue.2017.02.014.

[7] S.J. Maddox, Fatigue Strength of Welded Structures, 2nd ed., Woodhead Publishing, 2002.

[8] W. Fricke, Recent developments and future challenges in fatigue strength assessment of welded joints, Proc. Inst. Mech. Eng. C J. Mech. Eng. Sci. 229 (2014) 1224–1239, https://doi.org/10.1177/0954406214550015.

[9] N.E. Dowling, Mechanical Behaviour of materials: Engineering Methods for deformation, Fracture, and Fatigue, 4th ed., Pearson, 2012.

[10] D. Radaj, C.M. Sonsino, W. Fricke, Fatigue Assessment of Welded Joints by Local Approaches, 2nd ed., Woodhead Publishing, Cambridge, 2006.

[11] M. Braun, J.H. Grimm, H. Hoffmeister, S. Ehlers, W. Fricke, Comparison of fatigue strength of post-weld improved high strength steel joints and notched base material specimens, Ships Offshore Struct. 13 (2018) 47–55, https://doi.org/10.1080/17445302.2018.1425522.

[12] M.S. da Silva, D. Souza, E.H. de Lima, K.E. Bianchi, L.O. Vilarinho, Analysis of fatigue-related aspects of FCAW and GMAW butt-welded joints in a structural steel, J. Braz. Soc. Mech. Sci. Eng. 42 (2019), https://doi.org/10.1007/s40430-019-2142-8.

[13] J.D.M. Costa, J.A.M. Ferreira, L.P.M. Abreu, Fatigue behaviour of butt welded joints in a high strength steel, Procedia Eng. 2 (2010) 697–705, https://doi.org/10.1016/j.proeng.2010.03.075.

[14] C.M. Sonsino, T. Bruder, J. Baumgartner, S-N lines for welded thin joints-suggested slopes and FAT values for applying the notch stress concept with various reference radii, Weld. World 54 (2013) R375–R392, https://doi.org/10.1007/bf03266752.

[15] M. Stoschka, M. Leitner, G. Posch, W. Eichlseder, Effect of high-strength filler metals on the fatigue behaviour of butt joints, Weld. World 57 (2012) 85–96, https://doi.org/10.1007/s40194-012-0010-6.

[16] H. Remes, J. Romanoff, I. Lillemäe, D. Frank, S. Liinalampi, P. Lehto, P. Varsta, Factors affecting the fatigue strength of thin-plates in large structures, Int. J. Fatigue 101 (2017) 397–407, https://doi.org/10.1016/j.ijfatigue.2016.11.019.

[17] E. Harati, L. Karlsson, L.E. Svensson, K. Dalaei, Applicability of low transformation temperature welding consumables to increase fatigue strength of welded high strength steels, Int. J. Fatigue 97 (2017) 39–47, https://doi.org/10.1016/j.ijfatigue.2016.12.007.

[18] M.J. Ottersböck, M. Leitner, M. Stoschka, W. Maurer, Analysis of fatigue notch effect due to axial misalignment for ultra-high-strength steel butt joints, Weld. World 63 (2019) 851–865, https://doi.org/10.1007/s40194-019-00713-4.

[19] P. Schaumann, M. Collmann, Influence of weld defects on the fatigue resistance of thick steel plates, Procedia Eng. 66 (2013) 62–72, https://doi.org/10.1016/j.proeng.2013.12.062.

[20] L.W. Tong, L.C. Niu, Z.Z. Ren, X.L. Zhao, Experimental investigation on fatigue behaviour of butt-welded high-strength steel plates, Thin Walled Struct. 165 (2021), https://doi.org/10.1016/j.tws.2021.107956.

[21] G.K. Ahiale, Y.J. Oh, Microstructure and fatigue performance of butt-welded joints in advanced high-strength steels, Mater. Sci. Eng. A Struct. Mater. Prop. Microstruct. Process. 597 (2014) 342–348, https://doi.org/10.1016/j.msea.2014.01.007.

[22] S. Liinalampi, H. Remes, J. Romanoff, Influence of three-dimensional weld undercut geometry on fatigue-effective stress, Weld. World (2018), https://doi.org/10.1007/s40194-018-0658-7.

[23] M.J. Ottersböck, M. Leitner, M. Stoschka, Characterisation of actual weld geometry and stress concentration of butt welds exhibiting local undercuts, Eng. Struct. 240 (2021), https://doi.org/10.1016/j.engstruct.2021.112266.

[24] I. Weich, J. Lorenz, A. Fischl, S. Rodic, J. Buschner, Prüfungen im großen Maßstab, Stahlbau 81 (2012) 203–211, https://doi.org/10.1002/stab.201201531.

[25] C.M. Sonsino, Effect of residual stresses on the fatigue behaviour of welded joints depending on loading conditions and weld geometry, Int. J. Fatigue 31 (2009) 88–101, https://doi.org/10.1016/j.ijfatigue.2008.02.015.

[26] M. Braun, A.S. Milaković, F. Renken, W. Fricke, S. Ehlers, Application of local approaches to the assessment of fatigue test results obtained for welded joints at sub-zero temperatures, Int. J. Fatigue 138 (2020), https://doi.org/10.1016/j.ijfatigue.2020.105672.

[27] H. Remes, W. Fricke, Influencing factors on fatigue strength of welded thin plates based on structural stress assessment, Weld. World 58 (2014) 915–923, https://doi.org/10.1007/s40194-014-0170-7.

[28] F.V. Lawrence, J.D. Burk, R.J. Mattos, Y. Higashida, D. Hoeppner, Estimating the fatigue crack initiation life of welds. Fatigue Testing of Weldments, ASTM International, West Conshohocken, PA, 1978, pp. 134–158.

[29] T. Nykänen, T. Björk, R. Laitinen, Fatigue strength prediction of ultra-high strength steel butt-welded joints, Fatigue Fract. Eng. Mater. 36 (2013) 469–482, https://doi.org/10.1111/ffe.12015.

[30] T. Nykänen, T. Björk, Assessment of fatigue strength of steel butt-welded joints in as-welded condition – alternative approaches for curve fitting and mean stress effect analysis, Mar. Struct. 44 (2015) 288–310, https://doi.org/10.1016/j.marstruc.2015.09.005.

[31] M. Aguiari, M. Palombo, C.M. Rizzo, Performance characterisation of high-strength steel and quenched and tempered steels and their joints for structural applications, Weld. World 65 (2021) 289–300, https://doi.org/10.1007/s40194-020-01019-6.

[32] DNVGL-RP-C203: Recommended practice for fatigue design of offshore steel structures. (2016).

[33] I. Lillemäe, H. Remes, S. Liinalampi, A. Itävuo, Influence of weld quality on the fatigue strength of thin normal and high strength steel butt joints, Weld. World 60 (2016) 731–740, https://doi.org/10.1007/s40194-016-0326-8.

[34] M. Braun, R. Scheffer, W. Fricke, S. Ehlers, Fatigue strength of fillet-welded joints at subzero temperatures, Fatigue Fract. Eng. Mater. 43 (2020) 403–416, https://doi.org/10.1111/ffe.13163.

[35] M. Braun, Assessment of Fatigue Strength of Welded Steel Joints at Sub-Zero Temperatures Based on the Micro-Structural Support Effect Hypothesis, Technische Universität Hamburg, 2021, https://doi.org/10.15480/882.3782 [Doctoral Thesis].

[36] EN 1011-2:2001, Welding - Recommendation for Welding of Metallic Materials - Part 2: Arc welding of Ferritic Steels, Brussels, Belgium, 2001.

[37] DNVGL-OS-C401: Fabrication and testing of offshore structures. (2018).

[38] ISO 9015-1:2001, Destructive Tests on Welds in Metallic Materials-Hardness Testing-Part 1: Hardness Test on Arc Welded Joints, Geneva, Switzerland, 2001.

[39] J. Schubnell, M. Jung, C.H. Le, M. Farajian, M. Braun, S. Ehlers, W. Fricke, M. Garcia, A. Nussbaumer, J. Baumgartner, Influence of the optical measurement technique and evaluation approach on the determination of local weld geometry parameters for different weld types, Weld. World 64 (2020) 301–316, https://doi.org/10.1007/s40194-019-00830-0.

[40] F. Renken, R.U.F. von Bock und Polach, J. Schubnell, M. Jung, M. Oswald, K. Rother, S. Ehlers, M. Braun, An algorithm for statistical evaluation of weld toe geometries using laser triangulation, Int. J. Fatigue 149 (2021), https://doi.org/10.1016/j.ijfatigue.2021.106293.

[41] M. Braun, L. Kellner, S. Schreiber, S. Ehlers, Prediction of fatigue failure in small-scale butt-welded joints with explainable machine learning, Procedia Struct. Integr. (2021). Submitted for Publication.

[42] EN ISO 5817:2014 Welding - fusion welded joints in steel, nickel, titanium and their alloys (beam welding excluded) - Quality levels for imperfections. Brussels, BE, (2014).

[43] M. Braun, A.S. Milaković, S. Ehlers, A. Kahl, T. Willems, M. Seidel, C. Fischer, Sub-zero temperature fatigue strength of butt-welded normal and high-strength steel joints for ships and offshore structures in arctic regions, in: Proceedings of the ASME 39th International Conference on Ocean, Offshore and Arctic Engineering, Fort Lauderdale, FL, USA, 2020. OMAE2020-18892.

[44] M. Braun, A. Kahl, T. Willems, M. Seidel, C. Fischer, S. Ehlers, Guidance for material selection based on static and dynamic mechanical properties at sub-zero temperatures, J. Offshore Mech. Arct. Eng. 143 (2021) 1–45, https://doi.org/10.1115/1.4049252.

[45] A.F. Hobbacher, Recommendations for Fatigue Design of Welded Joints and Components, 2nd ed., Springer International Publishing Switzerland, 2016.

[46] T. Nykänen, T. Björk, A new proposal for assessment of the fatigue strength of steel butt-welded joints improved by peening (HFMI) under constant amplitude tensile loading, Fatigue Fract. Eng. Mater. 39 (2016) 566–582, https://doi.org/10.1111/ffe.12377.

[47] E. Niemi, W. Fricke, S. Maddox, Structural Hot-Spot Stress Approach to Fatigue Analysis of Welded Components, 2nd ed., Springer, Singapore, 2018.

[48] I. Lillemäe, H. Lammi, L. Molter, H. Remes, Fatigue strength of welded butt joints in thin and slender specimens, Int. J. Fatigue 44 (2012) 98–106, https://doi.org/10.1016/j.ijfatigue.2012.05.009.

[49] M. Braun, A.S. Milaković, G. Andresen-Paulsen, W. Fricke, S. Ehlers, A novel approach to consider misalignment effects in assessment of fatigue tests, Ship Technol. Res. (2020). Submitted for Publication.

[50] A. Ahola, T. Björk, Z. Barsoum, Fatigue strength capacity of load-carrying fillet welds on ultra-high-strength steel plates subjected to out-of-plane bending, Eng. Struct. 196 (2019), 109282, https://doi.org/10.1016/j.engstruct.2019.109282.

[51] B. Gaspar, Y. Garbatov, C.G. Soares, Effect of weld shape imperfections on the structural hot-spot stress distribution, Ships Offshore Struct. 6 (2011) 145–159, https://doi.org/10.1080/17445302.2010.497052.

[52] Z.G. Xiao, K. Yamada, A method of determining geometric stress for fatigue strength evaluation of steel welded joints, Int. J. Fatigue 26 (2004) 1277–1293, https://doi.org/10.1016/j.ijfatigue.2004.05.001.

[53] W. Fricke, A. Kahl, Comparison of different structural stress approaches for fatigue assessment of welded ship structures, Mar. struct. 18 (2005) 473–488, https://doi.org/10.1016/j.marstruc.2006.02.001.

[54] A. Ahola, T. Björk, Fatigue strength of misaligned non-load-carrying cruciform joints made of ultra-high-strength steel, J. Constr. Steel Res. 175 (2020), https://doi.org/10.1016/j.jcsr.2020.106334.

[55] R.U.F. von Bock und Polach, A. Kahl, M. Braun, H. von Selle, S. Ehlers, Analysis of governing parameters on the fatigue life of thermal cut edges, in: Proceedings of

the International Conference on Ships and Offshore Structures ICSOS 2019, Cape Carnival, USA, 2019.
[56] M. Braun, C. Fischer, J. Baumgartner, M. Hecht, I. Varfolomeev, Fatigue crack initiation and propagation relation at notched specimens with welded joints characteristics, Metals (2021) to be submitted shortly.
[57] W. Fricke, IIW Recommendations for the Fatigue Assessment of Welded Structures by Notch Stress analysis: IIW-2006-09, Woodhead Publishing, Cambridge, 2012.
[58] M.M. Pedersen, O.Ø. Mouritsen, M.R. Hansen, J.G. Andersen, J. Wenderby, Re-analysis of fatigue data for welded joints using the notch stress approach, Int. J. Fatigue 32 (2010) 1620–1626, https://doi.org/10.1016/j.ijfatigue.2010.03.001.
[59] K. Rother, W. Fricke, Effective notch stress approach for welds having low stress concentration, Int. J. Press. Vessels Pip. 147 (2016) 12–20, https://doi.org/10.1016/j.ijpvp.2016.09.008.
[60] M. Collmann, P. Schaumann, Querbelastete Stumpfstöße als kritisches Kerbdetail bei Stahlrohrtürmen und Monopiles, Stahlbau 87 (2018) 888–896, https://doi.org/10.1002/stab.201810016.
[61] H. Neuber, Kerbspannungslehre Grundlagen für genaue Festigkeitsberechnung mit Berücksichtigung von Konstruktionsform und Werkstoff, 2nd ed., Springer, Berlin, Heidelberg, 1958.
[62] R.E. Peterson, N. Sensitivity, G. Sines, J. Lwaisman, Metal Fatigue, McGraw-Hill, New York, 1959, pp. 293–306.
[63] D. Taylor, The Theory of Critical Distances: A New Perspective in Fracture Mechanics, Elsevier, 2007.
[64] D. Taylor, D. Hoey, High cycle fatigue of welded joints: the TCD experience, Int. J. Fatigue 31 (2009) 20–27, https://doi.org/10.1016/j.ijfatigue.2008.01.011.
[65] J. Baumgartner, H. Schmidt, E. Ince, T. Melz, K. Dilger, Fatigue assessment of welded joints using stress averaging and critical distance approaches, Weld. World 59 (2015) 731–742, https://doi.org/10.1007/s40194-015-0248-x.
[66] Z. Hu, F. Berto, Y.S. Hong, L. Susmel, Comparison of TCD and SED methods in fatigue lifetime assessment, Int. J. Fatigue 123 (2019) 105–134, https://doi.org/10.1016/j.ijfatigue.2019.02.009.
[67] M. Braun, A.M. Müller, A.S. Milaković, W. Fricke, S. Ehlers, Requirements for stress gradient-based fatigue assessment of notched structures according to theory of critical distance, Fatigue Fract. Eng. Mater. 43 (2020) 1541–1554, https://doi.org/10.1111/ffe.13232.
[68] M. Braun, A.S. Milaković, S. Ehlers, Fatigue assessment of welded joints at sub-zero temperatures by means of stress averaging approach, Ships Offshore Struct. 16 (2021) 216–224, https://doi.org/10.1080/17445302.2021.1906194.
[69] J. Baumgartner, H.C. Yıldırım, Z. Barsoum, Fatigue strength assessment of TIG-dressed welded steel joints by local approaches, Int. J. Fatigue 126 (2019) 72–78, https://doi.org/10.1016/j.ijfatigue.2019.04.038.
[70] M. Braun, J.H. Grimm, A.S. Milaković, H. Hoffmeister, A. Canaletti, S. Ehlers, W. Fricke, Bewertung der schwingfestigkeit ausgeschliffener schweißnähte aus hochfesten stählen und vergleich mit gekerbten grundmaterialproben, in: Proceedings of the 19 Tagung Schweißen in der maritimen Technik und im Ingenieurbau, Hamburg, Germany, 2019.
[71] S. Liinalampi, H. Remes, P. Lehto, I. Lillemae, J. Romanoff, D. Porter, Fatigue strength analysis of laser-hybrid welds in thin plate considering weld geometry in microscale, Int. J. Fatigue 87 (2016) 143–152, https://doi.org/10.1016/j.ijfatigue.2016.01.019.
[72] J. Baumgartner, Review and considerations on the fatigue assessment of welded joints using reference radii, Int. J. Fatigue 101 (2017) 459–468, https://doi.org/10.1016/j.ijfatigue.2017.01.013.
[73] M.L. Williams, Stress distribution at the base of a stationary crack, J. Appl. Mech. 24 (1956) 109–114.
[74] P. Lazzarin, R. Tovo, A notch intensity factor approach to the stress analysis of welds, Fatigue Fract. Eng. Mater. Struct. 21 (1998) 1089–1103, https://doi.org/10.1046/j.1460-2695.1998.00097.x.
[75] P. Livieri, P. Lazzarin, Fatigue strength of steel and aluminium welded joints based on generalised stress intensity factors and local strain energy values, Int. J. Fract. 133 (2005) 247–276, https://doi.org/10.1007/s10704-005-4043-3.
[76] G. Meneghetti, P. Lazzarin, Significance of the elastic peak stress evaluated by FE analyses at the point of singularity of sharp V-notched components, Fatigue Fract. Eng. Mater. Struct. 30 (2007) 95–106, https://doi.org/10.1111/j.1460-2695.2006.01084.x.
[77] G. Meneghetti, A. Campagnolo, F. Berto, Fatigue strength assessment of partial and full-penetration steel and aluminium butt-welded joints according to the peak stress method, Fatigue Fract. Eng. Mater. 38 (2015) 1419–1431, https://doi.org/10.1111/ffe.12342.
[78] G. Meneghetti, A. Campagnolo, State-of-the-art review of peak stress method for fatigue strength assessment of welded joints, Int. J. Fatigue 139 (2020), https://doi.org/10.1016/j.ijfatigue.2020.105705.
[79] H. Mettänen, T. Nykänen, T. Skriko, A. Ahola, T. Björk, Fatigue strength assessment of TIG-dressed ultra-high-strength steel fillet weld joints using the 4R method, Int. J. Fatigue 139 (2020), https://doi.org/10.1016/j.ijfatigue.2020.105745.
[80] A. Ahola, A. Muikku, M. Braun, T. Björk, Fatigue strength assessment of ground fillet-welded joints using 4R method, Int. J. Fatigue 142 (2021), https://doi.org/10.1016/j.ijfatigue.2020.105916.
[81] A. Ahola, T. Skriko, T. Björk, Fatigue strength assessment of ultra-high-strength steel fillet weld joints using 4R method, J. Constr. Steel Res. 167 (2020), https://doi.org/10.1016/j.jcsr.2019.105861.